

Numerical Study of Jet Impingement Heat Transfer on A Roughened Flat Plate

Alenezi A.H.¹, Abdulrahman Almutairi², Hamad M. Alhajeri³ and Addali A⁴

¹Mechanical Power and Refrigeration Department, College of Technological Studies, Shuwaikh, Kuwait

²Mechanical Power and Refrigeration Department, College of Technological Studies, Shuwaikh, Kuwait

Abstract. The purpose of this research paper is to investigate the effect of surface roughness on heat transfer. This was achieved by investigating the heat transfer in two cases: a smooth, horizontal surface (the baseline case) and the same surface with a roughness element added to it. The roughness elements took the shape of cubical pin-fin. The roughness element was further investigated by varying its height and width (e by e) to study their impact on the average Nu. Results are presented in the form of average Nusselt number \overline{Nu} within and beyond the stagnation region. Each roughness element was arranged in a circle concentric with the geometric centre (i.e. centre of jet) with a radius of one and a half jet diameters ($R/D = 1.5$). The jet diameter kept constant for all simulations ($D=13.5\text{mm}$) where the plane was located at $H/D = 6$ below the jet, for all the tests with a jet Reynolds number of 20,000 and jet temperature is 20° . The cubical pin-fin was tested for six different heights (e) from 0.25 mm to 1.50 mm in incremental steps of 0.25 mm for jet angle (α) of 90° .

1 Nomenclature

| | | |
|-----------------|---|-------------------------------|
| D | = | Jet diameter (m) |
| R | = | radial distance (m) |
| e | = | element height and width (m) |
| α | = | jet angle ($^\circ$) |
| Re | = | Reynold's number |
| Nu | = | local Nusselt number |
| r/D | = | dimensionless radial distance |
| \overline{Nu} | = | average Nusselt number |

2 Introduction

Jet Impingement cooling is a complex technique introduced into GT blade cooling in the early 1960's and has proven to be very effective for increasing the heat transfer rate compared to other cooling techniques. It is applied mostly on the inner surface of the blade through small holes in the inner passages to directly impinge on the hot regions such as blade leading edge. Kanokjaruvijit, and Martinez-botas [1],[2] added dimples to the surface of the target plate to examine the effect of jet impingement on a surface with a staggered array of dimples. They tested two dimpled geometries: cusped elliptical shape and hemispherical shape. The combined coupling effect of jet impingement and channel flow with the presence of cross-flow provided the highest heat transfer performance of the dimpled plate at large jet to plate spacing. At moderate cross-flow, either the channel flow or jet impingement could dominate the heat transfer

rate. At low cross-flow, jet impingement was found to be the dominant heat transfer mechanism. With the presence of dimples, flow circulation inside the concave dimples reduced heat transfer, especially with the smaller jet to plate spacing.

Zhang, et. al. [3] in his experimental and numerical studies employed an orthogonal single jet on a protrusion heated surface (constant heat flux). The protrusion took a shape of spherical pin-fin with height (δ) and diameter (D). Results were reported for local Nu distributions for Re 5000, 10,000 and 23000 and for normalized protrusion heights (δ/D) of 0.1,0.2 and 0.3. In general, flow structures are not effected by both protrusion depth or jet Reynolds number. A diversion in flow direction occurs when the flow meets with the protrusion and low pressure wake area behind the rib occurs where its length depends on the protrusion height. Overall, distributions of local Nu show higher magnitude for roughened surface when compared to smooth surface.

Kim, and Lee [4] conducted an experimental study of heat transfer and fluid flow characteristics of water drop impingement on a heated porous surface. They tested four different porous surfaces based on permeability and surface roughness obtained by using different sizes of small glass beads. Their test demonstrated two primary regions of impingement: contact and non-contact regions. The contact region is considered as water drop evaporation or boiling when in contact with the surface. The non-contact region is a surface film boiling regime where the drop was suspended in the air. The effects of

wall temperature, impact velocity and particle size of the porous substrate on thermal and fluid flow performances were investigated.

Celik [5] compared a smoothed and roughened the heated surface with co-axial jet impingement. The co-axial jet was a double pipe arrangement. This study concluded that the co-axial jet gave higher heat transfer than a single circular jet and that rough surface promoted better heat transfer due to interruption of the boundary layer over the roughened plate. The roughened surface achieved up to 27% higher averaged Nusselt number using the co-axial jet compared to a single circular jet configuration.

3 Numerical setup

3.1 Computational domain and boundary conditions

Figure 1 shows the axisymmetric computational domain and boundary conditions used in this simulation. The domain length and Radius which include the heated impingement surface (also referred to in the literature as “wall”) is 20D. An axisymmetric assumption is made to save computational time and cost; thus, we need to consider only one half of the domain shown in the figure. A separate simulation was carried out to provide the velocity profile on the domain inlet to ensure a fully developed flow based on the Reynolds number used in this simulation.

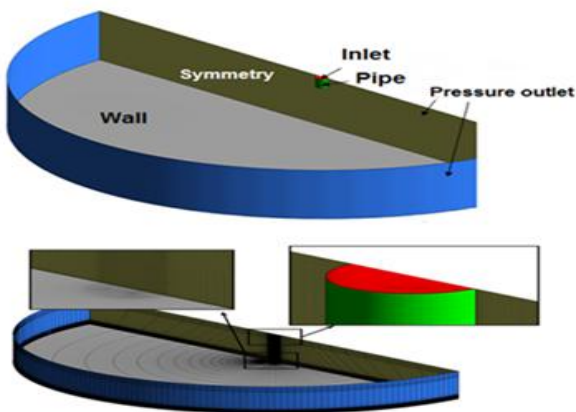


Figure 1. Geometry, boundary conditions, and grid for an orthogonal jet impingement.

3.2 Mesh generation, turbulence modelling and fluid properties

Figure 2 below shows an array of cubical pin-fins with detailed mesh for one of them. The array has also radius R of 1.5D measured from the geometric centre. The same as the case of spherical pin fin, a fixed distance of 1.3mm kept between all elements with varying their number to a maximum of 50 roughness elements when $e=0.25\text{mm}$, all have same width and height of e . The maximum percent increase in total surface area by using cubical pin-fin is 0.5%

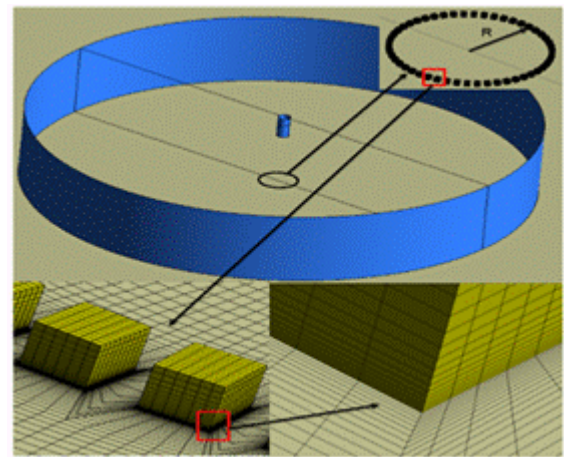


Figure 2. Computational mesh for a square cross-sectional pin-fin roughness element on a plane wall

The detailed geometry of all cubical pin-fins is shown in table 1.

Table 1. Detailed geometry for cubical pin-fin

| Height e (mm) | Area (mm^2) (5 faces) | Pitch (mm) | No. of roughness elements |
|-----------------|----------------------------------|------------|---------------------------|
| 0.25 | 0.3125 | 2.3 | 30 |
| 0.5 | 1.25 | 2.05 | 30 |
| 0.75 | 2.8125 | 1.79 | 30 |
| 1 | 5 | 1.55 | 30 |
| 1.25 | 7.8125 | 1.3 | 30 |
| 1.5 | 11.25 | 1.05 | 30 |

4 Results and discussion

4.1 Grid refinement study

This section shows the validation of the 3D- the axisymmetric model used in this simulation against the benchmark experimental result of O’Donovan and Murray [6].

Generally, both numerical solution accuracy and computational time depend primarily on mesh refinement. A suitable grid is one which has an acceptable run-time and good accuracy. A grid analysis was used in this research paper to certify that the solution is independent of the computational grid where three grid cases were used in the grid refinement study as shown in table 2 below.

Table 2. Detailed geometry for cubical pin-fin

| № | Size, cells | Y+ |
|--------|-------------|-----|
| Mesh 1 | 400 000 | 0.5 |
| Mesh 2 | 986 000 | 0.5 |
| Mesh 3 | 1 783 000 | 0.5 |

The commercial tool Ansys Fluent 16.2 was employed in this study to simulate the jet impingement. Extra attention was taken on the near-wall region since it plays an important role for convective heat transfer. The SIMPLEC scheme and Green-Gauss Cell Based gradient for spatial discretization were employed in this study using second order discretization schemes energy and momentum equations to produce more accurate results for heat transfer where first order schemes were used for other equations. Several steps were used before finalizing the choice of the appropriate solution: first, the use of the entire domain initialized by the inlet flow conditions employing first order upwind discretization to reach a convergence criterion at 10^{-6} for energy equation and 10^{-4} for the rest. The second step is seeking the solution by mixing up different orders of discretization schemes.

Figure 3 shows the simulated local Nusselt number varied with the radial distance (r/D) using the RNG $k-\epsilon$ turbulence model, for different grids and $\alpha=90^\circ$. The numerical results were compared against the experimental benchmark work of [6]. It is notable, that both experimental and the numerical local Nusselt number values are close to all grid cases and therefore, mesh 2 was adopted for the remaining numerical calculations.

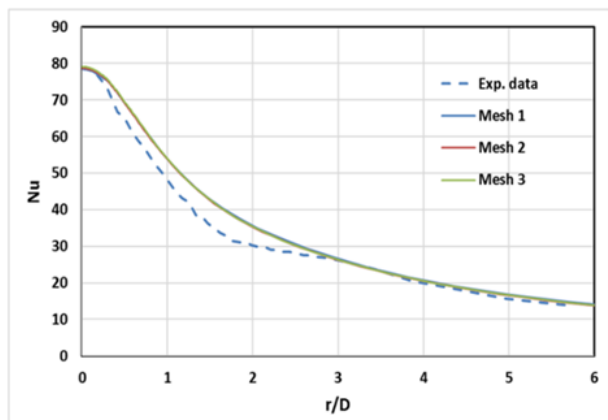


Figure 3. Local Nusselt number distribution for three grids, $H/D=6$, $Re=10,000$, $\alpha=90^\circ$

4.2 Average heat transfer performance

Figure 4 shows the effect of cubical height on the local Nusselt number distribution for a circular jet impinging on a flat plate. The cubical roughness element has a length and a width of e . Overall, two peaks of local Nu are shown for all heights due the flow recirculation occurs in front and after the roughness elements. Both peaks increase as the height increases so the drop in local Nu which occurs in the region attached to the roughness wall. At $r/D \approx 2.25$, and $e \leq 0.75$ mm, all local Nu curves starts to match as the height variation is no more affects the heat transfer rate. However, for $e \geq 1$ mm, curves of roughened surfaces show a slight lower value of local Nu than the smooth case.

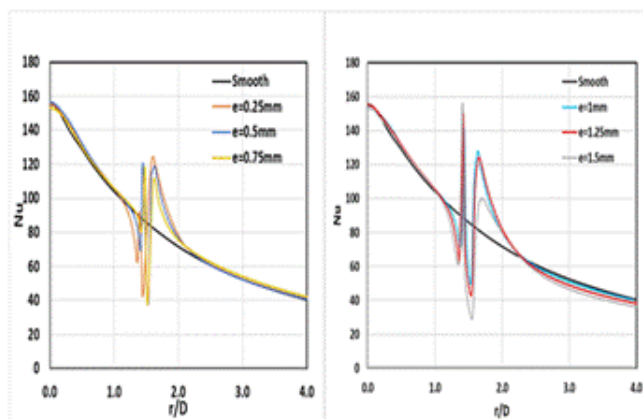


Figure 4. Effect of cubical pin-fin height on local Nusselt number for $Re=20,000$, $H/D=6$ and $\alpha=90^\circ$.

Local Nu contours are shown in Figure 5 below. Overall, cubical pin-fins show higher local heat transfer distributions for all heights. As e increases, so does the local heat transfer rate, this is obvious for $0.25\text{mm} \leq e \leq 1.25\text{mm}$. However, for $e=1.5\text{mm}$, Nu starts to fall due to the increase of the wake region behind the roughness element. This low-pressure region forces the flow to recirculate within it which effects the main flow velocity by reducing it. This reduction causes heat transfer rate to diminish.

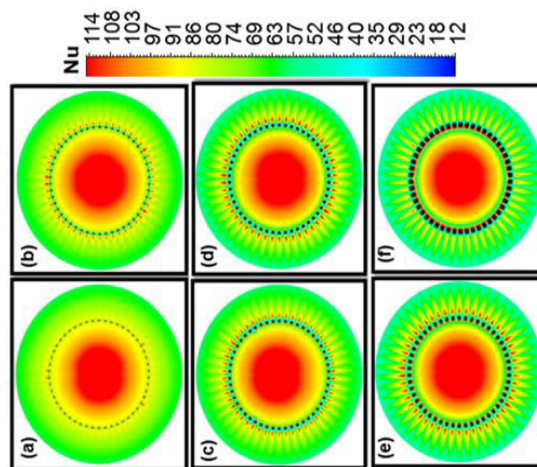


Figure 5. Local Nu contours for roughness heights of (a) 0.25 mm, (b) 0.5 mm, (c) 0.75 mm, (d) 1mm, (e) 1.25mm and (f) 1.5 mm, $Re=20,000$, $H/D=6$ and $\alpha=90^\circ$.

To identify the low-pressure zone behind the roughness element, contours of velocity vectors of three cubical pin fins heights are shown in figure 6 below. The figure shows velocity vector contours for three pin heights; 0.25 mm, 0.75 mm and 1.5 mm. As shown in the figure, the higher the pin, the larger the separation region (the region above the fin top edge), the larger the low-pressure region, and the higher the local Nu. However, for $e=1.5$ mm, flow starts to recirculate above the top edge of fin, as shown in the figure, causing the main jet to travel a longer distance and reducing its arrival velocity before it hits the heated surface resulting lowest increase in \overline{Nu} .

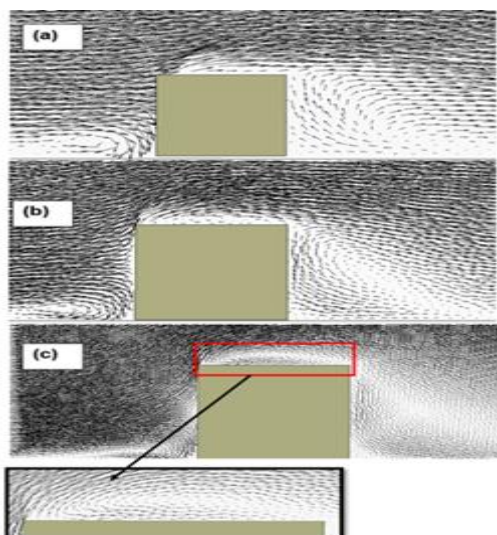


Figure 6. Contours of velocity vectors for heights (a) $e=0.25\text{mm}$, (b) $e=0.75\text{mm}$ and (c) $e=1.5\text{mm}$, $Re=20,000$, $H/D=6$ and $\alpha = 90^\circ$

Figure 7 below shows the effect of using a cubical pin-fin on \overline{Nu} . The figure shows that, \overline{Nu} can vary by up to about 7.2% of the value of the smooth surface, for the smaller pin heights (0.25 mm and 0.5 mm) but gradually decreasing to about -1.4% for $e=1.5$ mm. The rate of heat transfer increases as the tip of the square pin-fin gets closer to the jet exit since the surface area is increased. However, as the fin height further increases, both velocity and pressure of the jet decreases causing the average Nu over the surface area to diminish but the local Nu which is based only on the local value may increase [7].

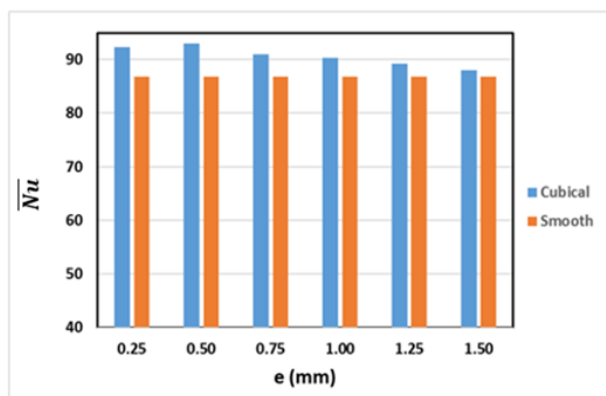


Figure 7. Effect of cubical pin-fin height on average Nusselt number over $0 \leq r/D \leq 4$, $Re= 20,000$, $H/D=6$

5 Conclusion

The research paper reports the results of using simulation to investigate the effects on the average predicted Nu, of cubical pin-fins imposed on a flat, horizontal plane (the wall) subject to flow of cold fluid from a nozzle of diameter 13.5mm. The roughness element was located at the same radial distance measured from the geometric centre, $R/D=1.5$ on a plane located $H/D=6$. The optimum

height of the spherical pin-fins was investigated using six heights; 0.25 mm to 1.50 mm in increments of 0.25 mm, for jet angle ($\alpha=90^\circ$).

The maximum enhancement of \overline{Nu} was obtained by the use cubical pin-fin roughness elements with height (e) of 0.5 mm with 7.2% percentage increase comparing to the smooth case. The minimum enhancement percentage of the average Nu was 1.4% when employing cubical pin-fins with the maximum height (e) of 1.5mm. The enhancement percentages vary with changing the roughness element height and width.

6 References

1. Kanokjaruvijit, K., Martinez-Botas, R. F. Jet impingement on a dimpled surface with different crossflow schemes. *International Journal of Heat and Mass Transfer*. 2005; 48(1): 161–170.
2. Kanokjaruvijit, K., Martinez-Botas, R. F. Heat Transfer and Pressure Investigation of Dimple Impingement. *ASME Conference Proceedings*. 2005; 2005: 717–728.
3. Zhang D., Qu H., Lan J., Chen J., Xie Y. Flow and heat transfer characteristics of single jet impinging on protrusioned surface. *International Journal of Heat and Mass Transfer*. Elsevier Ltd; 2013; 58(1–2): 18–28.
4. Kim, W., S., Lee, S. Y. Behavior of a water drop impinging on heated porous surfaces. *Experimental Thermal and Fluid Science*. Elsevier Inc.; 2014; 55: 62–70.
5. Celik, N. Effects of the surface roughness on heat transfer of perpendicularly impinging co-axial jet. *Heat and Mass Transfer/Waerme- und Stoffuebertragung*. 2011; 47(10): 1209–1217.
6. O'Donovan, T., S., Murray, B. D. Jet impingement heat transfer - Part I: Mean and root-mean-square heat transfer and velocity distributions. *International Journal of Heat and Mass Transfer*. 2007; 50(17–18): 3291–3301.
7. Sanyal, A., Srinivasan, K., Dutta P. Numerical study of heat transfer from pin-fin heat sink using steady and pulsated impinging jets. *IEEE Transactions on Components and Packaging Technologies*. 2009; 32(4): 859–867.